Rare Metal Materials and Engineering
Volume 49, Issue 7, July 2020
Available online at www.rmme.ac.cn

Science Press

Cite this article as: Rare Metal Materials and Engineering, 2020, 49(7): 2240-2249

ARTICLE

Recent Advances for Interface Diffusion Behavior in *M*CrAlY Coatings at Elevated Temperature Oxidation

Yang Hongzhi[1, 2], **Zou Jianpeng**[1], **Shi Qian**[2], **Lin Songsheng**[2], **Dai Mingjiang**[2], **Wang Di**[2]

[1] State Key Laboratory of Powder Metallurgy, Central South University, Changsha 410083, China; [2] Guangdong Institute of New Materials, National Engineering Laboratory for Modern Materials Surface Engineering Technology, Key Lab of Guangdong for Modern Surface Engineering Technology, Guangzhou 510651, China

Abstract: *M*CrAlY coatings are playing an important role in protecting the Ni-based superalloy substrate from oxidation and corrosion at high temperature, which can form dense and continuous oxide scales on the surface to retard the diffusion of cations and oxygen. The oxide scale is mainly composed of by α-Al_2O_3 of high thermal and chemical stabilities as well as the low diffusivity of oxygen and metal ions in its hexagonal close-packed (HCP) structure. The concentration of aluminum in the coating near coating/oxide scales interface decreases with the depletion of Al for the growth of alumina layer, which further suppresses the consecutive Al_2O_3-scale growth, causing the formation of mixed oxide compounds and cracks as well as voids. Also, accompanied with the interface diffusion behavior, the microstructure of the oxide scales evolves due to the changes of the chemical composition, which makes a significant influence on the oxidation resistance property of the coating. At elevated temperature, the coating/Ni-based superalloy interface diffusion process will make deleterious effects because of its thermally activated nature and the difference in chemical composition. The inward diffusion of Al from the Al-rich coating and the outward diffusion of Ni from the Ni-rich superalloy, accompanied with the phase transformation from γ-Ni phase to γ'-Ni_3Al phase, will result in an interdiffusion zone (IDZ). Furthermore, the phase transformation will result in a secondary reaction zone (SRZ), which mainly consists of refractory element-rich topologically close-packed (TCP) phases, such as σ, μ and Laves phases. These TCP phases with dendritic nature of solidification in the matrix may reduce the high-temperature fatigue life of the Ni-based superalloy. The interface diffusion process of *M*CrAlY coatings is addressed in this paper, together with a summary of current understanding of the effects accompanied with the interface diffusion. This work can help to understand the microstructure change and element diffusion behavior of the *M*CrAlY coatings in the oxidation process, which has guiding significance for improving the oxidation resistance and understanding the failure mechanism of the coatings.

Key words: *M*CrAlY coating; interface diffusion; IDZ; SRZ

*M*CrAlY (*M*: Ni, Co or Ni+Co) coatings with good high temperature properties are widely used as standalone coatings to protect the substrate from oxidation and corrosion at high temperature. These protecting coatings can form dense and continuous oxide scales on the surface to retard the diffusion of cations and oxygen. They can be also used as bond coats in thermal barrier coating (TBC) systems to improve the physical compatibility and adhesion between substrate and top ceramic coat[1,2]. The *M*CrAlY coatings usually contain (wt%) 15~25 Cr, 10~15Al and 0.2~0.5Y, and consist of β-NiAl phase in γ-Ni matrix. Depending on the temperature and coating composition, the microstructure of the coating may be more

---

Received date: July 12, 2019
Foundation item: Scientific Research Fund of Guangdong Province (2016A030312015); GDAS' Special Project of Science and Technology Development (2017GDAS CX-0202); Natural Science Foundation of Hunan Province (2018JJ2524); Guangdong Science and Technology Program (2017A070701027); GDAS' Project of Science Technology Development (2017GDASCX-0111); Guangdong Science and Technology Plan Project (2014B070705007)

Corresponding Author: Zou Jianpeng, Ph. D., Professor, State Key Laboratory of Powder Metallurgy, Central South University, Changsha 410083, P. R. China, Tel: 0086-731-88876630, E-mail: zoujp@csu.edu.cn

complex, containing other phases, like γ'-Ni_3Al, α-Cr, and σ-(Co,Cr) phases[3]. Generally, in the composition of the *M*CrAlY coatings, Al and Cr elements play an important role in oxidation and corrosion resistance performance. Because of the dense oxide of α-Al_2O_3 and Cr_2O_3, the diffusion of oxygen into the interior of the coating will be inhibited, reducing the degradation of the substrate. This stable α-Al_2O_3 with equiaxed crystal structure is considered as the most effective protective film against oxidation due to its lower oxygen-diffusion rate compared with other oxides. And higher content of Al could also significantly inhibit the formation of spinel oxides[4]. γ'-Cr_2O_3 will form in the initial stage of oxidation and then transform into the α-Cr_2O_3 at the temperature of 300 °C to 600 °C. The α-Cr phase formed after isothermal oxidation can reduce the thermal expansion coefficient of the bond coat, which is beneficial to extend the service life of the coating. And Cr could also reduce the critical value of Al content required to form an effective Al_2O_3 protective film[5]. Y is the most important reactive element in *M*CrAlY coatings, because it can modify alumina growth mechanisms and promote the adhesion between oxide scales and matrix, effectively improving the static and cyclic oxidation resistance of the coating[6]. In further oxidation process, Y_2O_3 will react with Al_2O_3 to form $AlYO_3$ and $Al_5Y_3O_{12}$, named YAG, and improve the coating oxidation resistance and interlayer adhesion through the effect of pinning[7]. Also, it can suppress the segregation of harmful elements, such as S in the grain boundary and the diffusion of Al along the lattice. Thereby the oxidation rate can be reduced and the service life of the coating can be extended[8].

*M*CrAlY coatings could be prepared by a number of processes including electron beam-physical vapor deposition (EB-PVD)[9], low pressure plasma spraying (LPPS)[10], vacuum plasma spraying (VPS)[11], atmospheric plasma spraying (APS)[12], high velocity oxygen fuel (HVOF) spraying[13], and arc ion plating (AIP)[14]. PVD and VPS could offer high quality coating for minimal oxidation and well controlled composition during deposition, providing flexibility in depositing coatings of various chemical compositions.

The durability and reliability of advanced *M*CrAlY coating are critically related to its oxidation behavior. Ideal *M*CrAlY coatings should oxidize to form a slow-growing, nonporous, and adherent α-Al_2O_3 scale layer, which were affected by the coatings composition, microstructure and surface condition[15]. Continuous and dense α-Al_2O_3 scale layer is preferred because of its high thermal and chemical stabilities as well as the low diffusivity of oxygen and metal ions in its hexagonal close-packed (hcp) structure. With the depletion of Al for the further growth of α-Al_2O_3 and spallation, the Al content in the alloy will reach a critically low value that can no longer sustain the continued growth of the protective scale. Consequently, less protective oxides, like fast-growing Ni(Co, Cr)-spinels, are formed, which reduces the coating life[16]. In addition, the interdiffusion with the substrate needs to be minimized to reduce the Al depletion and external diffusion of the matrix elements, avoiding the formation of second reaction zone (SRZ). During the service, the interdiffusion process between the coating and substrate is also acknowledged as one of the key factors for coating failure. Interdiffusion inevitably occurs through coating/substrate interface at high temperature and leads to microstructure evolution, due to the alloying element gradient between *M*CrAlY coatings and superalloy substrates. Such microstructural changes at coating/substrate interface may affect the mechanical behavior of the coating-substrate system. So it's worthwhile to discuss in more detail the interface diffusion process during the high temperature oxidation.

1 Oxidation Behavior of *M*CrAlY Coatings

Under service at high temperature, the *M*CrAlY coatings are exposed to an oxidation condition to form a compact oxide scales, providing a high oxidation resistance and protecting the substrate from further oxidation. The oxidation behavior of *M*CrAlY coatings can be quantitatively revealed by the growth kinetics of the oxide scales according to the conventional Wagner oxidation theory.

In the initial stage of oxidation, the oxide scales are mainly transient θ-Al_2O_3, the growth of which is mainly depended on the outward diffusion of Al, causing a rapid mass increasing. At this stage, the oxidation rate is very high, supported by the large slope of the oxidation kinetic curve as shown in Fig.1, named the linear growth regime[7]. The linear law may be caused by the formation of micro-cracks within the scales due to the thermal stress and growth stress or comprehensive effects of complex oxide scales, of which the rate-controlling step is a metal-oxygen reaction at the interface between the oxide scales and the coating[17]. In such cases, the growth rate is independent to the thickness of the coating:

$$\frac{dx}{dt} = k_0 \tag{1}$$

with k_0 being a constant. Integration gives

$$x=x_0+k_0t \tag{2}$$

where x_0 is the initial scale thickness at t=0. Linear rate laws have been observed when the oxide scales are not protective, as in the case of alkali metals, and in oxidation in weak oxidation environments such as dilute oxygen or mixtures of CO and CO_2 [18].

The formation and growth of α-Al_2O_3 layer can suppress the formation of unprotected oxides and spinels, which retards the further penetration of the oxygen, improving the high temperature oxidation resistance. Then the coating enters the steady-state oxidation stage, in which the oxidation rate drastically drops, playing an important role in determining the service life of the coating. During steady-state oxidation stage according to the Wagner oxidation theory (the parabolic

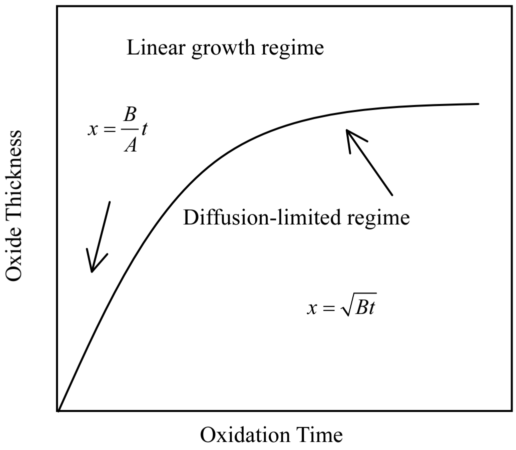

Fig.1 Oxidation kinetic curve of oxide layers[7]

law), the growth of the oxide scales is controlled by the high temperature diffusion of the elements and the oxide scales growth kinetics curves obey the parabolic law. It had been reported that for a relatively short oxidation time (no more than hundreds of hours), the experimental results of the weight gain and oxide scales thickness are basically in line with the parabolic law[19]. At this stage, the oxidation rate drops rapidly and its growth depends mainly on the diffusion process. The parabolic growth law of the oxide scales results from the diffusion-controlled growth mechanism. The scales growth rate can be easily deduced from Fick's law of diffusion. For example, if oxygen is the diffusion-controlling species, Fick's law of diffusion provides $J=-D\ \mathrm{d}c/\mathrm{d}x$, where D is the diffusivity and $\mathrm{d}c/\mathrm{d}x$ is the concentration gradient for the diffusing species.

This equation can be rewritten in terms of weight gain w and thickness x as Eq.(3):

$$\mathrm{d}w/\mathrm{d}t=-D\mathrm{d}c/\mathrm{d}x \qquad (3)$$

where $w=r'x$ for unit area of the cross section and r' is the oxide density. Rearranging the equation, we have

$$r'\frac{\mathrm{d}x}{\mathrm{d}t} = -D\frac{\mathrm{d}c}{\mathrm{d}x} = D\frac{\Delta c}{x} = D\Delta c\frac{\mathrm{d}t}{r} \qquad (4)$$

Here we have assumed a linear gradient so that $\mathrm{d}c/\mathrm{d}t=\Delta c/x$, where $\triangle c$ is the concentration change over distance x. Integrating $x\mathrm{d}x=D\mathrm{d}c\ \mathrm{d}t/r$ over x, increasing from 0 to x when time goes from 0 to t, we get

$$x^2=2D\Delta ct/r' \qquad (5)$$

Substituting $k=2D\Delta c/r'$, we get

$$x^2=kt \qquad (6)$$

The oxide scales growth depends on temperature and oxygen partial pressure. The temperature dependency appears through the diffusivity factor, which follows the relationship:

$$D=D_0\exp(-\Delta H/RT) \qquad (7)$$

where D_0 is a constant, R is the gas constant, ΔH is the activation energy of diffusion, and T is the temperature in Kelvins. As shown in Fig.1, the alumina grows predominantly by inward diffusion of anions along the oxide scales grain boundaries but there is a contribution to k by outward diffusion of cations. This outward growth appears to be sensitive to cations dissolved in the alumina[20].

2 Interface Diffusion Behavior

2.1 *M*CrAlY coatings/oxide scales interface diffusion behavior

It has been well recognized that the microstructure of the oxide scales is a decisive factor for the oxidation resistance of the coating[21]. During the initial oxidation stage of the *M*CrAlY coatings, also named the transient stage, the formed oxide composition and microstructure depend on the supply of the metal elements to the surface according to the Wagner's oxidation theory[22]. Because of the relatively high activity of Al to oxygen compared with Cr and Ni, the θ-Al_2O_3 is firstly formed on the surface with fast growing rate. Simultaneously, some Cr_2O_3 and NiO were also formed, sporadically distributed in the alumina layer[23]. The θ-Al_2O_3 is transient oxide and then will transform into α-Al_2O_3. The rate of the transformation from θ-Al_2O_3 to α-Al_2O_3 has a significant impact on oxide scales microstructure, which controls the overall growth rate of alumina scale at the initial oxidation stage. By the nucleation of α-Al_2O_3 at oxide/coating interface, α-Al_2O_3 grows outward by consuming transient oxides[24]. The existence of Cr can also accelerate this transformation. Furthermore, the formation of α-Al_2O_3 can suppress the formation of Cr_2O_3 and NiO, conversely. Finally, α-Al_2O_3 grows as a dense and continuous layer, becoming the dominant oxide. Once a continuous α-Al_2O_3 layer is formed, the subsequent oxidation will be controlled by diffusion through the α-Al_2O_3 layer, which can be supported by drastic drop of the oxidation rate constant[25]. Then the coating enters the steady-state oxidation stage, which plays an important role in the properties of the *M*CrAlY coatings, determining the service life of the coating. The interdiffusion process is also complex at this stage, making significant effect between the coating and substrate.

At higher temperature in the interface of the oxide scales and coating, diffusion is the dominant process because of its thermally activated nature and causes simultaneous outward and inward migrations of aluminum and oxygen, respectively. This reverse movement of aluminum and oxygen leads to the formation of aluminum oxide compound layer. The SEM image of the surfaces for the NiCoCrAlY coatings prepared by electron beam-physical vapor deposition (EB-PVD) in Fig.2a shows lace-like network morphology of α-Al_2O_3, implying a preferential diffusion of oxygen from oxide surface toward oxide/coating interface. Whereas, in Fig.2b, the NiCoCrAlY coatings with the same composition prepared by plasma activated electron beam-physical vapor deposition (PAEB-PVD) shows whisker-like morphology of θ-$A1_2O_3$, indicating the growth caused by the outward diffusion of Al[26]. θ-Al_2O_3 belongs to monoclinic crystal with defective spinel structure, which provides fast diffusion channels for the outward transportation of aluminum ions. However, the dominantly controlling mechanism for further growth of the α-Al_2O_3 is controversial, which is controlled by the inward transport of oxygen as well as by the outward diffusion of Al cations along the grain boundaries[27]. Based on the research of stress and performance of thermal barrier coatings (TBC), Jamnapara et al[28] and Fang et al[29] assumed that the diffusion of O controlled the growth of α-Al_2O_3 layers. However, Song et al[30] held that the growth of the α-Al_2O_3 layer was dominated by the diffusion of Al and Ni rather than O according to EBSD results. They also found the diffusion pathway of Al and Ni was along the pores and cracks, which promoted the further growth.

The transformation from θ-Al_2O_3 to α-Al_2O_3 is accompanied with the formation of cracks in the oxide scales, which provide more migration paths for the outward and inward diffusion. When oxygen encounters with metallic phases (such as β-NiAl, γ'-Ni_3Al) and solute atoms (such as Cr), they will react and form oxides owing to the high affinities of O with Al and Cr through the reactions as follows[31]:

$$4\beta\text{-NiAl}+3O_2\rightarrow 2\alpha\text{-}Al_2O_3+4[Ni] \quad (8)$$

$$4\gamma'\text{-}Ni_3Al+3O_2\rightarrow 2\alpha\text{-}Al_2O_3+12[Ni] \quad (9)$$

$$2[Al]+3[O]\rightarrow \alpha\text{-}Al_2O_3 \quad (10)$$

$$2[Cr]+3[O]\rightarrow \alpha\text{-}Cr_2O_3 \quad (11)$$

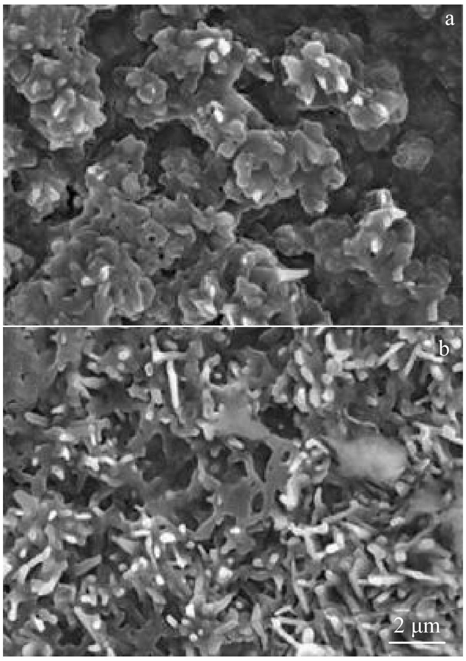

Fig.2 Surface SEM images of the NiCoCrAlY coatings after oxidation at 1373 K for 100 h by different manufacture methods: (a) EB-PVD and (b) PAEB-PVD[26]

The molar Gibbs free energies for formation of α-Al_2O_3 and α-Cr_2O_3 at 1100 ºC are –1328 kJ/mol and –763 kJ/mol, respectively[32]. Hence, α-Al_2O_3 can form under a lower oxygen partial pressure than Cr_2O_3. Additionally, at the beginning of oxidation, O rapidly reacts with Al, Cr and Ni on the coating surface to form an external oxide layer consisting of a mixture of Al_2O_3, Cr_2O_3, and NiO. With protection of the external oxide layer, penetration of O to the coating/substrate interface becomes difficult. So that the partial pressures of oxygen in the interface zone is too low to form Al_2O_3 and Cr_2O_3 simultaneously, and only high enough for O to react with Al to form α-Al_2O_3 layer. In this way, α-Al_2O_3 grows into a dense and continuous layer[33]. With depletion of Al during the oxidation, the residual oxygen concentration in the interface zone increases gradually and becomes high enough for formation of Cr_2O_3, then Cr_2O_3 starts to grow, forming an oxide layer with a local maximum thickness of about 5 μm at the coating/substrate interface shown in Fig.3a. Considering that the content of Cr (15wt%~25wt%) in the coating is greater than that of Al (10wt%~15wt%), Cr_2O_3 takes larger proportion of the interfacial oxide layer than α-Al_2O_3, so it can be well understood that why the interfacial oxide layer presents an upper Cr_2O_3 layer with large thickness and a lower α-Al_2O_3 layer with small thickness, as shown in Fig.3b[34]. In the vicinity of the oxides layer, some voids can be observed, which also facilitates the diffusion of both oxygen and other elements of the coatings.

The depletion of Al occurring in α-Al_2O_3 growth and interface diffusion process can decrease the concentration of aluminum in the coating, which further suppresses the consecutive Al_2O_3-scale growth. And O activity was increased with the oxidation severity, which could promote the localized detachment and/or micro-cracking, thus accelerate oxide-layer spallation[35]. And the oxide layer will split into two sub-layers. The one near the surface comprises a mixture of α-Al_2O_3, Cr_2O_3 and Ni(Al, $Cr)_2O_4$, while the other near the coating consists of dense α-Al_2O_3 and Cr_2O_3. Mercier et al[36] have studied the effect of the aluminum concentration on the oxidation behavior of the Ni-Al system. It was demonstrated that internal Al_2O_3 forms with external $NiAl_2O_4$ and NiO when the aluminum content is between 1wt%~6wt%. As a result, although diffusion through the Al_2O_3 scale is very slow as mentioned previously, an insufficient concentration in aluminum coupled with defects in the Al_2O_3 scale, causes Ni, Cr and Co ions to diffuse to the surface resulting in the formation of a mixed oxide layer. Chen et al[37] have reported that α-Cr_2O_3 and the (Ni, Co)(Cr, $Al)_2O_4$ spinel phase start to form when the Al concentration reaches a critical low value. Moreover, they make note of a reduction of the Al_2O_3 scale after aluminum depletion with the increase of the oxidation time. This can be attributed to the solid state reaction between the NiO and Al_2O_3 oxides which forms $NiAl_2O_4$. The formation of mixed oxide phases with high growth rate, such

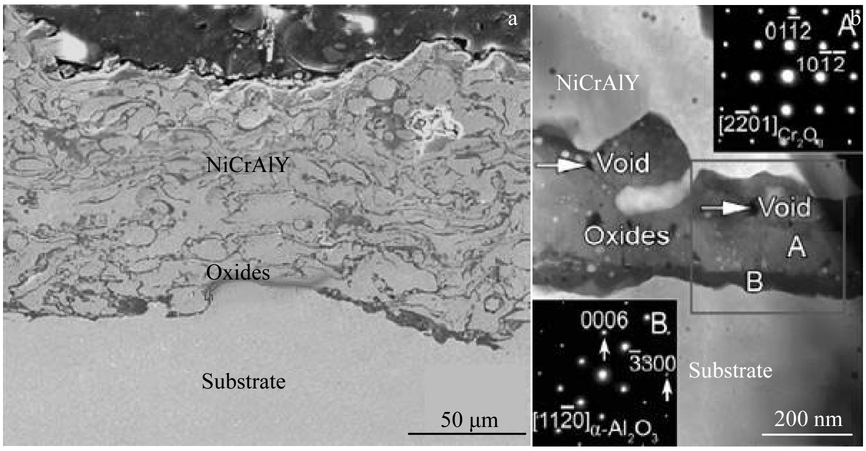

Fig.3 Cross-sectional microstructure of NiCrAlY coating after oxidation (a) and HAADF image of the interface between the coating and the substrate (b)[34]

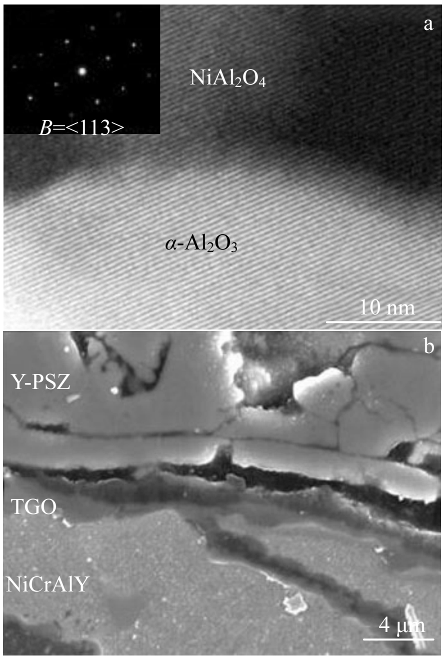

Fig.4 HRTEM image showing a detail of the interface between α-Al_2O_3 and $NiAl_2O_4$ spinels (a) and SEI showing spallation and cracking at the bond coat/top coat interface in the TBC oxidized at 1050 ℃ for 336 h (b)

as NiO, Cr_2O_3 and $Ni(Cr, Al)_2O_4$ spinels accelerates localized oxidation by providing fast oxygen diffusion paths. The detail for α-Al_2O_3 and $NiAl_2O_4$ spinel at the substrate/coating interface is shown in Fig.4a[38]. Then the coating enters the final stage, breakaway stage.

At the breakaway stage, the Al-rich phases such as β or γ', cannot be found. $NiAl_2O_4$ spinel was grown over α-Al_2O_3 particle, as shown in Fig.4a. Also, NiO was scarcely observed with the increase of the exposure time. The fast growth rate and associated volume changes lead to thermo-mechanical fatigue cracking along or close to the coating and the oxide scales interface, which promotes the spallation of the oxides layer from the coating, resulting in premature mechanical failure and thus severely limit the lifetime, as shown in Fig.4b. The new surface formed by shedding will enter the transient stage again. However, the oxidation resistance of the coating is reduced for the discontinuous oxide layer. The big cracks shown in Fig.4b reduces the adhesion of the ceramic top coat and bond coat. Also, the cracks extending into the interior of the coating facilitate the penetration of oxygen, accelerating the failure of the coating.

The stability of oxide product phases that formed during oxidation may be rationalized by constructing thermodynamic stability diagrams of Ni-Al-O system, which describes the equilibrium between the phases in this system (Al_2O_3, $NiA1_2O_4$, NiO and Ni-A1 alloys), as shown in Fig.5[39]. Because of the high affinities of O with Al as well as the high oxygen partial pressure on coating surface at initial stage, Al-riched alumina scale firstly forms and continues to grow. Then, with depletion of Al for further oxidation, the residual oxygen concentration in the interface zone decreases gradually, which is hard to form alumina. Because of the protection by α-Al_2O_3 layer, the penetration of O in coatings becomes difficult. Upon alumina growth, as the aluminum activity decreases, conversely, the oxygen activity at the interface increases along line (1). When a_O reaches the intersection of lines (1) and (2), the $A1_2O_3$ will convert to $NiA1_2O_4$ according to the following reaction[40]. When this happens, the durability of the coating may be compromised, as mentioned above. Seriously, the $NiA1_2O_4$ spinels will further convert to NiO. With the fast growth and associated volume changes, cracks will be induced in the vicinity of the $NiA1_2O_4$ spinels and NiO, which are beneficial for the penetration of the oxygen.

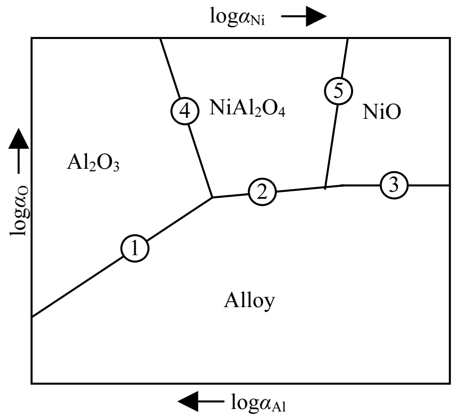

Fig.5 Thermodynamic stability diagram of Ni-Al-O system[39]

$$3Ni+4Al_2O_3 \rightarrow 3NiAl_2O_4+2Al \quad (12)$$

$$3Ni+NiAl_2O_4 \rightarrow 4NiO+2Al \quad (13)$$

2.2 Substrate/*M*CrAlY coatings interface diffusion behavior

Interdiffusion between the coating and the underlying Ni-based superalloy substrate inevitably occurs during thermal exposure at high temperature. Since *M*CrAlY coatings usually have a higher Cr and Al content than the Ni-based superalloy substrates for promoting the formation of protective oxide scales, conversely, the Ni-based superalloy substrates have a greater content of Ni, Ti and refractory elements like Ta, W, Mo and Re mainly for improving the high temperature mechanical properties. The interdiffusion process can cause the loss of protective oxides forming elements of the coating and the formation of harmful brittle phases in the substrate[41]. It has been widely reported that a secondary reaction zone (SRZ) accompanied with much detrimental topologically close-packed (TCP) phases formed in the substrate owing to the interdiffusion, which caused the local chemistry changes in the substrate as shown in Fig.6a[42, 43]. And the TCP phases such as μ, σ, and P phases are principally composed of the elements Ni, Co, Cr, W, Mo and Re. Generally, Ni, Cr and Re partitioned strongly to σ phase and W, Mo and Co concentrated in μ phase. The high density of TCP phases generally present needle like or rod like morphology, as shown in Fig.6b[44].

For advanced Ni-based single crystal superalloys, the addition of refractory elements such as W, Re and Mo aims to reinforce their creep or stress rupture strength at elevated temperature[45]. The 3rd generation Ni-based single crystal (SC) superalloy contains high concentrations of rhenium (Re), the content of which is up to about 6 wt% to improve again the high temperature capability and creep strength. Recently the 4th generation Ni-based SC superalloy has achieved further thermal stability and remarkable creep strength by the addition of ruthenium (Ru)[46]. The addition of these elements keeps the substrate too much prone to the precipitation of TCP phases and secondary reaction zone during the service at high temperature above 1100 °C[47]. TCP phases are typically characterized in the form of 'basket weave' sheets, which are aligned with the octahedral planes in the fcc matrix[48]. According to the analysis of EDS, the TCP phases are principally composed of high levels of refractory elements, such as W, Re, Cr and Co, while low levels of Al because of the interdiffusion between the coating and the substrate as well as the depletion of Al[49]. It is suggested that SRZ is derived from the local compositional changes due to diffusion of Al and other elements between the coating layer and the substrate.

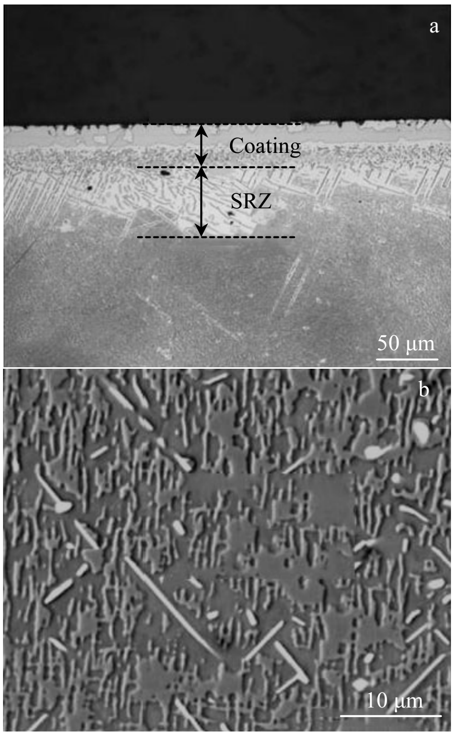

Fig.6 A SRZ between the coating and the Ni-based superalloy (a)[42] and BSE images of cross-section morphology of SRZ after thermal cyclic oxidation (b)[44]

The inward diffusion of Al, Cr, Co and outward diffusion of W, Re causes the formation of unstable γ/γ' phase. The transformation, which is driven by local reductions in chemical free energy and, in some cases, strain energy, occurs through a combined mechanism of boundary precipitation and interfacial migration. High angle grain boundaries in polycrystalline alloys and defects such as freckles in single crystal alloys serve as sites for heterogeneous nucleation of precipitates and also as high diffusivity mobile reaction fronts[50]. Cr which diffuses from the coating to the substrate is not solid dissolved in the in γ/γ' phase, but precipitates in the form of α-Cr. Actually, the solid solubility of the refractory elements is much lower in β phase than in γ/γ' phase, and they will precipitate when the phase transitions from γ/γ' phase to β phase occur owing to the diffusion of Al from coating to matrix[51].

The growth of SRZ is supposed to be dominantly controlled by the inward diffusion of aluminum from the coating layer to the substrate. The Al activity of the coating and the residual stress state of the coating surface play an important role in determining the propensity of a specimen to form SRZ. The outward diffusion of Ru from the substrate to the coating layer may also contribute to SRZ formation. The presence of TCP phases will consume the alloy solid solution reinforcing elements, which will reduce the mechanical properties of the matrix, especially the creep and rupture properties[52].

2.3 Effect of interface diffusion behavior

2.3.1 Residual stress

Accompanied with the growth of the oxide scales and the interdiffusion process, the residual stress during the oxidation should not be neglected. The thickness and crystallography of the oxide scales, especially the alumina, are critical to achieve reproducible coatings life and prevent premature spallation[40]. For example, a complex strain in the oxide scales will be caused by the increase in the thickness during its exposure to high-temperatures, or thermal cyclic conditions, which produces much stress near the oxide scales region. Also, the oxide scales are the major source of strain which primarily derives the cracking, delamination and spallation of the top coating from the bond coat surface. In addition, it has been observed that during thermal exposure, the residual stress increases as the oxide scales grows, which would accelerate the spallation process of the coating[53]. The increased thickness of the oxide scales can result in constrained volume expansion, leading to in-plane compressive growth stresses. Also, thermal compressive residual stresses in the oxide scales for the thermal expansion mismatch with the substrate can reach about 3~6 GPa[54]. During thermal cycling, the oxide scales will relieve compression by means of out-plane displacements, preferentially into the coating, thus causing the creep deformation. During repeated thermal cycling, progressive roughening of the coating/oxide scales interfaces occurs as shown in Fig.7[55]. The rough surface presented as undulations, which also referred to rumpling or ratcheting.

2.3.2 Crack propagation

The crack propagation is also related to the growth and coalescence of oxide-induced cracking, connecting with pre-existing discontinuities in the oxide scales and coating, which appears to be controlled by the oxide scales growth during thermal cycling. The depletion of Al can lead to the phase transformations such as β to γ' and/or martensite formation (for a β-NiAlPt bond coat), which generates large stresses contributing factors in promoting undulation growth. At the same time, the loss of Al changes the *M*CrAlY coatings properties, creating voids at the coating/substrate interface.

2.3.3 Decrease of thermal cycling performance

Several of the concurrent mechanisms operating related to the temperature and thermal cycling during engine service are schematically depicted in Fig.7 (reproduced from Clarke and Levi)[56, 57]. The stresses in the oxide scales exert a central influence during the coating service life, which mainly come from thermal expansion coefficients (TEC) misfit and the other from oxide scales growth. These stresses play an important role in thermal cycling[58, 59]. Based on the above consideration for the TEC misfit and growth stresses, the oxide scales experienced large in-plane compression during thermal cycling. As a result, the buckling and visco-plastic deformation of the bond coat formed through out-plane displacements to alleviate these stresses and associated strain energy density, as dark gray wavy strip shown in Fig.7. These displacements induce tensile σ_{zz} stresses normal to the interface that motivate delamination mechanisms. When imperfections exist around the oxide scales, the cracks would nucleate and grow in this vicinity by the induction of the tension, and then the coalescence of these cracks leads to failure[60, 61].

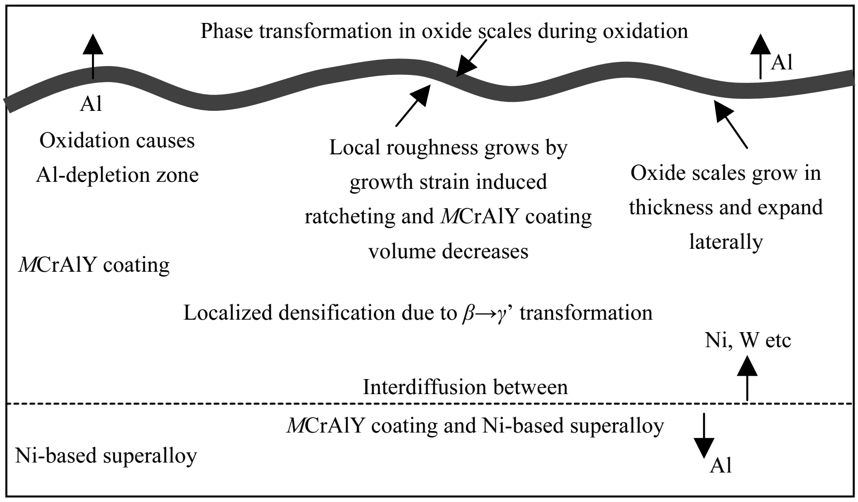

Fig.7 Schematic summary of the several of the concurrent processes occurring in the high temperatures[56,57]

2.4 Efforts for reducing interface diffusion process

As mentioned above, the interdiffusion between the coating and the substrate will become a serious problem at high temperature, which can promote the precipitation of detrimental phases in the substrate. In addition, inward diffusion of Al into the substrate and the growth of the alumina layer could result in Al depletion and finally degrade the oxidation resistance in long-term thermal exposure[62]. So efforts had been done to reduce the process, such as addition of rare earth elements (RE) in the coating and building diffusion-barrier between the coating and substrate[63].

The RE with excellent chemical activity delivers great potential for improving the microstructure of the alloy and increasing the oxidation resistance. Over the last two decades, the effects of the elements additions (Y, Hf, Zr, Si, Pt and Re) had been studied extensively[64, 65]. With the addition of the RE to the *M*CrAlY coatings, the adhesion of the alumina scales can be improved. The diffusion rate of Al and Cr elements was reduced, which can depress the consumption rate of protective elements thus prolonging the service life of *M*CrAlY coatings[66]. It was reported by He et al[67] that the addition of Dy brings a lower oxide scale growth rate and better bonding of scales. The addition of Re[68] or Ta[69] also enhances coating oxidation performance by lowering the oxidation rate and Al diffusivity. Ru addition in *M*CrAlY coatings improved long-term oxidation performance by reducing substrate interdiffusion[70]. Pt addition reduced voids formation near oxide/coating interface, improving cyclic oxidation resistance[71]. Some RE additions bring obvious beneficial effect, whereas others can have a disastrous influence on the oxidation properties. Though numerous hypotheses have been proposed in order to explain the beneficial effect of reactive elements, no clear defined model was proposed to explain it completely[72].

Another feasible way is to design thin diffusion barrier, such as refractory metals[73,74], intermetallic[75], and ceramics[76] between coating and substrate. Extensive efforts have been made to suppress or postpone the diffusion of alloying elements by various types of diffusion barrier coatings. The study conducted by Cheng et al[77] reported the use of an ion plated-Cr_2O_3 intermediate film as a diffusion barrier between the NiCrAlY coating and the γ-TiAl substrate. This layer by the formation of two continuous Al-rich oxide films at both TiAl/Cr_2O_3 and Cr_2O_3/NiCrAlY interfaces, suppressed the inward diffusion of the Ni from the NiCrAlY coating to the γ-TiAl substrate. Guo et al[78] also reported that the gradient oxide dispersed (OD) NiCoCrAlY coating produced by electron beam-physical vapour deposition (EB-PVD) not only could improve a lower oxidation rate, but also could increase the TGO adherence because the outward diffusion of elements such as Ta, W, and Hf from the superalloy effectively blocked by the OD zone.

Recently, studies focus on ceramic-based diffusion barriers owing to outstanding elemental diffusion resistance and good high-temperature thermal stability. Wang et al[79] reported that the yttria partially stabilized zirconia (YSZ) coating as a diffusion barrier significantly improved the oxidation resistance of the NiCrAlY coating due to the inhibition of the interdiffusion of alloying elements. Their results indicate that the YSZ coating as a diffusion barrier reacted with Al from the NiCrAlY coating and the superalloy substrate to form two adherent Al_2O_3 layers thereby preventing the interdiffusion between the coating and the substrate effectively. AlN diffusion barrier, which can effectively inhibit the interdiffusion between coating and substrate, is considered as a potential candidate for diffusion barrier layer[80]. Zhu et al[81] used an AlN interlayer deposited by the filtered vacuum arc evaporation as a diffusion barrier between the Ni+CrAlYSiHfN composite coating and the K417G superalloy. Their results indicate that the AlN diffusion barrier prevented the interdiffusion between the coating and the substrate effectively after 200 h exposure at 1000 °C.

Extensive efforts have been made to suppress or postpone the diffusion during the oxidation process. It has been proposed that the proper pre-treatment of the *M*CrAlY coat under a low oxygen partial pressure, before isothermal oxidation, is an effective way to lower the growth rate of oxide scales, since a thin and continuous α-Al_2O_3 layer forms on the surface[82].

3 Summary

1) *M*CrAlY coatings provide protection of Ni-based superalloys used in aero-engine and gas turbine engines against oxidative attack and hot gas corrosion because of the formation of a slowly growing, continuous and adherent α-Al_2O_3 layer under service conditions. Thus the high-temperature mechanical properties of nickel-base superalloys can be maintained with longer time and the degradation process in the aggressive high temperature conditions can also be retarded.

2) Diffusion of elements between the *M*CrAlY coatings and the substrate is inevitable at the working temperature due to the thermally activated nature and chemical concentration gradient, which is detriment to both of them and brings residual stress, cracks propagation and decrease of its service life. The occurrence of interdiffusion decreases the concentration of aluminum in the coating, thereby reducing the ability of the coating to sustain exclusive Al_2O_3-scale growth, particularly in the event of localized detachment and/or microcracking, which can promote oxide-scale spallation. The formation of topologically close-packed (TCP) phases in the region of the original coating/substrate interface can be deleterious to the mechanical properties of the superalloy substrate.

3) Attempts, including the addition of rare earth elements and building diffusion-barrier between the *M*CrAlY coatings and Ni-based superalloys, have been made to prevent or limit

the interdiffusion between *M*CrAlY coatings and the substrates. And efforts should be carried out to study the effect of the addition of rare earth elements and effective diffusion barriers. Long term availability of the rare earth elements should also be concerned in the *M*CrAlY coatings industry application.

References

1 Perepezko J H. *Science*[J], 2009, 326(5956): 1068

2 Sun J, Fu Q G, Liu G N *et al*. *Ceramics International*[J], 2015, 41(8): 9972

3 Naeimi F, Rahimipour M R, Salehi M. *Oxidation of Metals*[J], 2016, 86(1-2): 59

4 Sirvent P, Cruz D, Múnez C J *et al*. *Journal of Thermal Spray Technology*[J], 2016, 25(4): 694

5 Lee C, Kim J. *Journal of Thermal Spray Technology*[J], 2015, 24(4): 592

6 Sun J, Jiang S M, Yu H J *et al*. *Corrosion Science*[J], 2018, 139(7): 172

7 Kim D, Shin I, Koo J *et al*. *Journal of Mechanical Science & Technology*[J], 2014, 28(2): 513

8 Gamm-Seminar, Hackbusch W, Wittum G. *Surface Technology* [J], 2014, 43(3): 152

9 Jackson R D, Taylor M P, Evans H E *et al. Oxidation of Metals*[J], 2011, 76(3-4): 259

10 Yanar N M, Kim G, Hamano S *et al*. *High Temperature Technology*[J], 2014, 20(4): 495

11 Fossati A, Ferdinando M D, Bardi U *et al*. *Journal of Thermal Spray Technology*[J], 2012, 21(2): 314

12 Waki H, Kitamura T, Kobayashi A. *Journal of Thermal Spray Technology*[J], 2009, 18(4): 500

13 Yuan K, Peng R L, Li X H *et al. Surface & Coatings Technology*[J], 2015, 261(1): 86

14 Guo M H, Wang Q M, Ke P L *et al*. *Surface & Coatings Technology*[J], 2006, 200(12): 3942

15 Task M N, Gleeson B, Pettit F S *et al. Oxidation of Metals*[J], 2013, 80(5-6): 541

16 Salam S, Hou P Y, Zhang Y D *et al. Corrosion Science*[J], 2015, 95(3): 143

17 Zhao P, Shen M, Gu Y *et al. Corrosion Science*[J], 2017, 126(9): 317

18 Sequeira C A C. *Uhlig's Corrosion Handbook*[M]. Hoboken: John Wiely & Song, Inc, 2011

19 Zhang B Y, Yang G J, Li C X *et al*. *Applied Surface Science*[J], 2017, 406(2): 99

20 Mao W G, Luo J M, Dai C Y *et al. Applied Surface Science*[J], 2015, 338(2): 92

21 Chęcmanowski J, Matraszek A, Szczygieł I *et al*. *Journal of Thermal Analysis & Calorimetry*[J], 2013, 113(1): 311

22 Chen Y, Zhao X F, Xiao P. *Acta Materialia*[J], 2018, 159(15): 150

23 Puetz P, Huang X, Yang Q *et al*. *Journal of Thermal Spray Technology*[J], 2011, 20(3): 621

24 Swadźba R, Swadźba L, Wiedermann J *et al*. *Oxidation of Metals*[J], 2014, 82(3-4): 195

25 Zhu C, Li P, Wu X Y. *Ceramics International*[J], 2016, 42(6): 7708

26 Peng H, Guo H, He J *et al*. *Surface & Coatings Technology*[J], 2012, 207(21): 110

27 Postolenko V. *Failure Mechanisms of Thermal Barrier Coatings for High Temperature Gas Turbine Components Under Cyclic Thermal Loading*[D]. Aachen: Aachen University, 2008

28 Jamnapara N I, Frangini S, Alphonsa J *et al*. *Surface and Coatings Technology*[J], 2015, 266(3): 146

29 Fang X, Zhang G, Feng X. *Ceramics International*[J], 2015, 41(2): 2840

30 Song X, Meng F, Kong M *et al*. *Vacuum*[J], 2016, 134(9): 33

31 Chen Y, Zhao X, Bai M *et al. Acta Materialia*[J], 2017, 128(4): 31

32 Yang L, Chen M, Wang J *et al*. *Corrosion Science*[J], 2017, 126(9): 344

33 Tang J J, Bai Y, Liu K *et al*. *Oxidation of Metals*[J], 2016, 86(1-2):75

34 Liu Y Z, Hu X B, Zheng S J *et al*. *Materials & Design*[J], 2015, 80(5): 63

35 Li X, Huang X, Yang Q *et al. Journal of Engineering for Gas Turbines & Power*[J], 2016, 138(1): 1229

36 Mercier D, Kaplin C, Goodall G *et al*. *Surface & Coatings Technology*[J], 2010, 205(7): 2546

37 Chen S F, Liu S Y, Wang Y *et al. Journal of Thermal Spray Technology*[J], 2014, 23(5): 809

38 Poza P, Gómez-García J, Múnez C J. *Acta Materialia*[J], 2012, 60(20): 7197

39 Mohammadreza D, Mat Y M A, Kay C M *et al. Corrosion Science*[J], 2018, 144(7): 13

40 Nayebpashaee N, Seyedein S H, Aboutalebi M R *et al*. *Surface & Coatings Technology*[J], 2016, 291(4): 103

41 Bai B, Guo H, Peng H *et al. Corrosion Science*[J], 2011, 53(9): 2721

42 Liang T, Guo H, Peng H *et al. Journal of Alloys & Compounds*[J], 2011, 509(34): 8542

43 Cheng K Y, Jo C Y, Jin T *et al. Journal of Alloys & Compounds*[J], 2011, 509(25): 7078

44 Rettig R, Singer R F. *Acta Materialia*[J], 2011, 59(1): 317

45 Shi L, Xin L, Wang X *et al. Journal of Alloys & Compounds*[J], 2015, 649(7): 515

46 Matsuoka Y, Aoki Y, Matsumoto K *et al*. *Superalloys*[J], 2004, 200(24): 637

47 Das D K, Gleeson B, Murphy K S *et al. Metal Science Journal*[J], 2013, 25(2): 300

48 Zhong J, Liu J, Zhou X *et al. Journal of Alloys & Compounds*[J], 2016, 657(2): 616

49 Wang D, Peng H, Gong S *et al. Corrosion Science*[J], 2014, 78(1): 304

50 Das D K, Gleeson B, Murphy K S *et al*. *Materials Science and Technology*[J], 2009, 25(2): 300

51 Das D K, Gleeson B, Murphy K S *et al. Metal Science Journal*[J], 2013, 25(2): 300

52 Zhong X, Zhao H, Zhou X *et al. Journal of Alloys & Compounds*[J], 2014, 593(593): 50

53 Zhang B Y, Yang G J, Li C X *et al. Applied Surface Science*[J], 2017, 406(2): 99

54 Cheruvu N S, Chan K S, Viswanathan R. *Energy Materials*[J], 2013, 1(1): 33

55 Mishra S K, Jagdeesh N, Pathak L C. *Journal of Materials Engineering & Performance*[J], 2016, 25(7): 2570

56 Sangalli D, Debernardi A. *Physical Review B*[J], 2011, 84(21): 2461

57 Fritscher K, Klaus F, Braue W *et al. Metallurgical & Materials Transactions A*[J], 2013, 44(5): 2070

58 Mema R, Yuan L, Du Q *et al. Chemical Physics Letters*[J], 2011, 512(1): 871

59 Chen H, Gao Y, Luo H *et al. Journal of Thermal Spray Technology*[J], 2011, 20(6):1201

60 Mishra S K, Jagdeesh N, Pathak L C. *Journal of Materials Engineering & Performance*[J], 2016, 25(7): 2570

61 Gao W, Li Z. *Developments in High-temperature Corrosion and Protection of Materials*[M]. Cambridge: CRC Press, 2008

62 Heuer A H, Nakagawa T, Azar M Z *et al. Acta Materialia*[J], 2013, 61(18): 6670

63 Pint B A. *Materials Science Forum*[J], 2011, 696(9): 57

64 Hu L, Hovis D B, Heuer A H. *Oxidation of Metals*[J], 2010, 73(1-2): 275

65 Yanar N M, Pettit F S, Meier G H. *Metallurgical & Materials Transactions A*[J], 2006, 37(5): 1563

66 Wang H Y，Zuo D W，Li X F *et al. Journal of Rare Earths*[J], 2010, 28(2): 246

67 He J, Zhang Z, Peng H *et al. Corrosion Science*[J], 2015, 98(9): 699

68 Salam S, Hou P Y, Zhang Y D *et al. Corrosion Science*[J], 2015, 95(7): 143

69 Pulci G, Tirillò J, Marra F *et al. Metallurgical & Materials Transactions A*[J], 2014, 45(3): 1401

70 Chen S F, Liu S Y, Wang Y *et al. Journal of Thermal Spray Technology*[J], 2014, 23(5): 809

71 Qi W, Peng H, He J *et al. Surface & Coatings Technology*[J], 2014, 259(11): 426

72 Darolia R. *International Materials Reviews*[J], 2013, 58(6): 315

73 Ma J, Jiang S M, Gong J *et al. Corrosion Science*[J], 2011, 53(9): 2894

74 Reddy K T, Cernansky N P, Cohen R S. *Journal of Propulsion & Power*[J], 2015, 5(1): 6

75 Szymański K, Hernas A, Moskal G *et al. Surface & Coatings Technology*[J], 2015, 268(4): 153

76 Guo C, Wang W, Cheng Y *et al. Corrosion Science*[J], 2015, 94(5): 122

77 Cheng Y X, Wang W, Zhu S L *et al. Intermetallics*[J], 2010, 18(4): 736

78 Peng H, Guo H, He J *et al. Journal of Alloys & Compounds*[J], 2010, 502(2): 411

79 Guo C, Wang W, Cheng Y *et al. Corrosion Science*[J], 2015, 94(5): 122

80 Ren P, Zhu S, Wang F. *Surface & Coatings Technology*[J], 2016, 286(6): 262

81 Ren P, Zhu S, Wang F. *Applied Surface Science*[J], 2015, 359(11): 420

82 Zhang B Y, Yang G J, Li C X *et al. Applied Surface Science*[J], 2017, 406(2): 99

*M*CrAlY 高温防护涂层界面扩散行为研究进展

杨洪志[1,2]，邹俭鹏[1]，石　倩[2]，林松盛[2]，代明江[2]，王　迪[2]

(1. 中南大学 粉末冶金国家重点实验室，湖南 长沙 410083)

(2. 广东省新材料研究所 现代材料表面工程技术国家工程实验室 广东省现代表面工程技术重点实验室，广东 广州 510651)

摘　要：*M*CrAlY 涂层在高温环境下可在涂层表面生成致密连续的氧化层，以阻止阳离子和氧离子的扩散，在保护镍基高温合金基体免受高温氧化和腐蚀方面发挥着重要作用。氧化层主要由 α-Al$_2$O$_3$ 组成，其具有较高的热稳定性和化学稳定性，同时在其六方密堆积（HCP）结构中氧离子和金属离子具有较低的扩散系数。随着氧化铝层的生长，使得涂层/氧化层界面铝浓度降低，进一步抑制了连续的 Al$_2$O$_3$ 层的生长，导致氧化层中形成混合氧化物和裂缝以及空隙。同时，伴随着界面扩散过程，使得氧化层的微观结构因化学成分的变化而转变，这将对涂层的抗氧化性能产生显著影响。在高温条件下，由于扩散的热活化特性及涂层与基体化学成分的差异，涂层/镍基合金基体界面扩散过程将对基体合金产生有害影响。此时，Al 会从涂层内扩散至基体合金中，同时 Ni 会从基体合金扩散至涂层中，使得基体合金的微观结构发生相转变（γ-Ni 相→γ'-Ni$_3$Al 相），形成互扩散区（IDZ）。镍基合金微观结构的相转变使得难熔元素析出，形成二次反应区（SRZ），其主要由富含难熔元素的拓扑密堆积（TCP）相组成，例如 σ、μ 和 Laves 相等，且具有枝状晶结构。因此，TCP 相的析出将会对镍基合金的高温疲劳寿命产生严重影响。本文综述了 *M*CrAlY 涂层界面扩散的详细过程，同时对界面扩散过程的影响进行了总结。这将有利于深入了解涂层在氧化过程中的组织结构变化和元素扩散行为，对提高涂层的高温抗氧化性能及研究涂层的失效机理具有借鉴意义。

关键词：*M*CrAlY 涂层；界面扩散；互扩散区；二次反应区

作者简介：杨洪志，男，1991 年生，博士，中南大学粉末冶金国家重点实验室，湖南 长沙 410083，电话：0731-88876630，E-mail: yanghz@csu.edu.cn